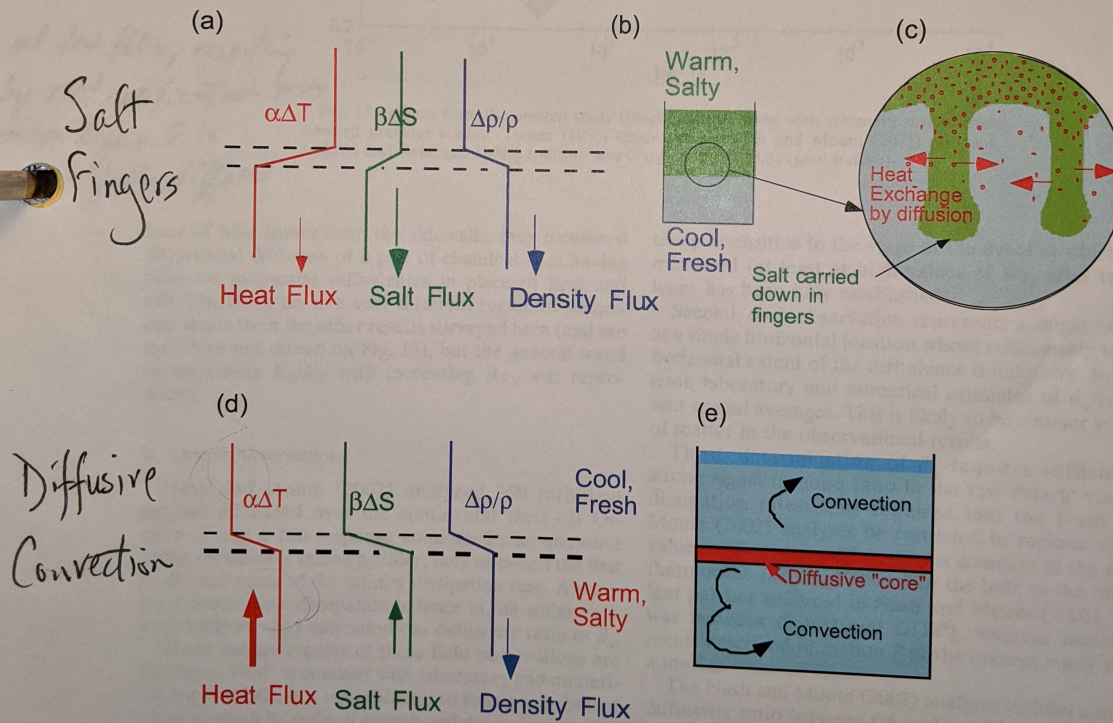


Double diffusion

Double Diffusion

Figure 2: (a) Background stratification (WS/CF) during a "rundown" salt-fingering experiment. The net fluxes, shown schematically as arrows, are proportional to the difference between the initial (dashed) and final (solid) profiles. (b) diagram of tank containing salt-finger interface between well-mixed layers (c Magnified view of salt-fingers showing the mechanism of the instability. (d) Background stratification (CF/WS) for a diffusive sense convection experiment, with a diffusive interface and well-mixed layers above and below. (e) diagram of tank showing convecting layers and diffusive interface.



Differential diffusion at low buoyancy Reynolds number

at small values of Re_b resorting by density stratification may occur before S is fully diffused

this is because S diffuses more slowly than T

$$d = K_S / K_T$$

$$Re_b = \varepsilon / vN^2 = (\ell_b / \eta)^{4/3}$$

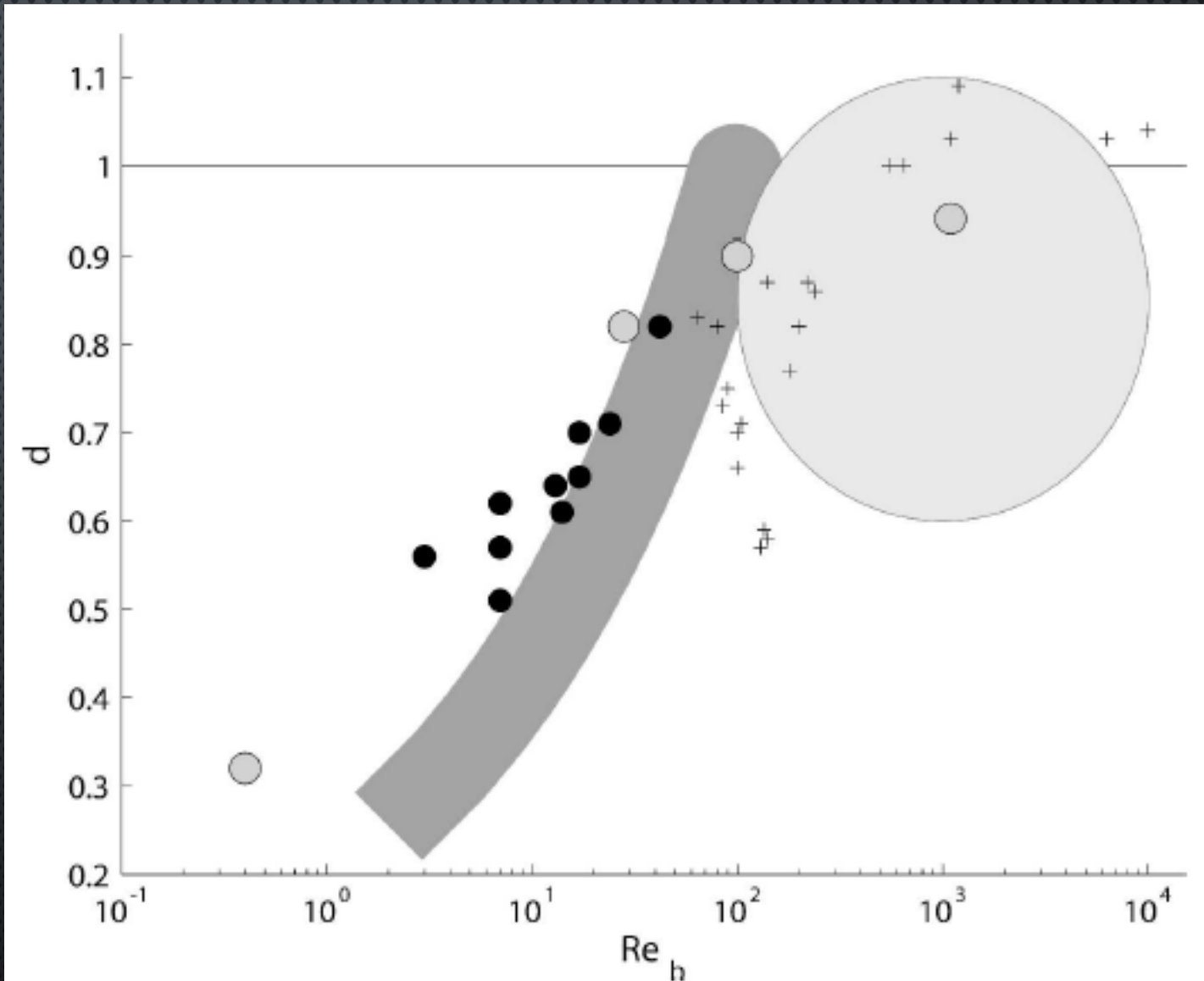


FIG. 15. Results from the present study (black bullets), along with summary results from selected previous studies: Turner (1968) (thick curve), Nash and Moum (2002) (ellipse), Jackson and Rehmann (2003) (pluses), and Gargett et al. (2003) (gray bullets).

$$\sigma = \frac{\gamma}{\chi}$$

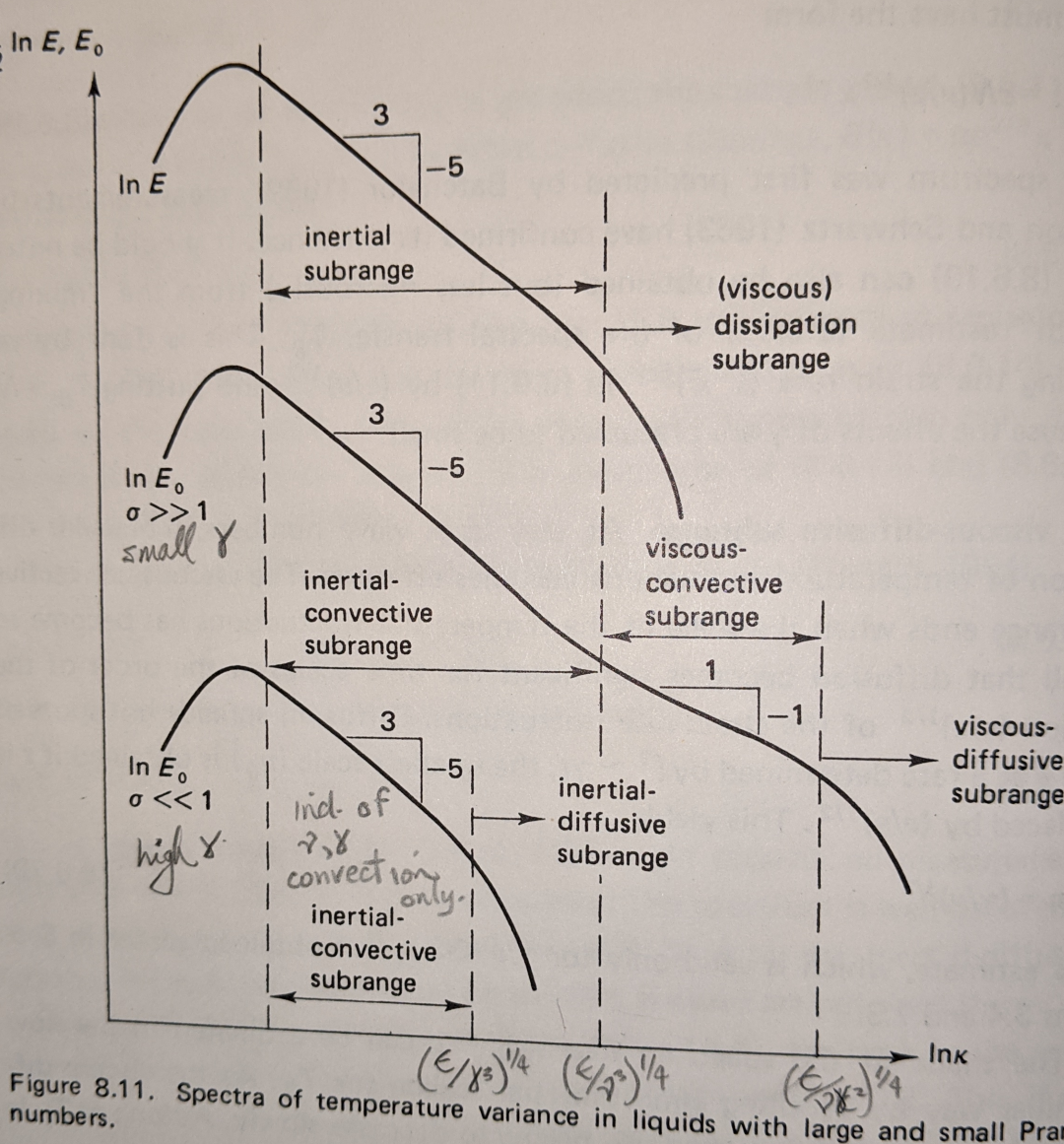


Figure 8.11. Spectra of temperature variance in liquids with large and small Prandtl numbers.

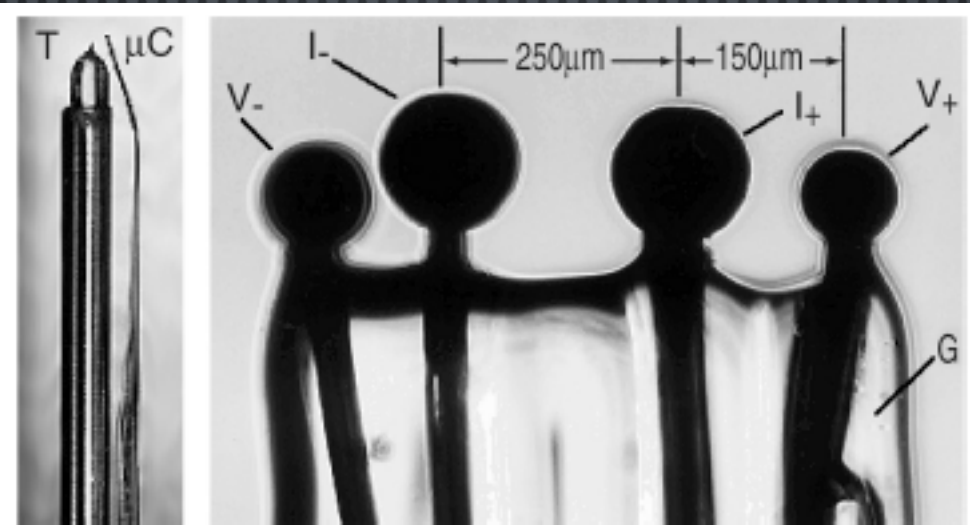


FIG. 2. A side view of the upper inch of the microconductivity-temperature (μ CT) probe (left, $2 \times$ mag). The fast-response FP07 microbead thermistor (T) is separated by 1 mm from the conductivity (μ C) tip, a cross section of which is shown at right, magnified $100\times$. The conductivity probe consists of two current-supplying (I_- , I_+) and two voltage-measuring spherical platinum electrodes (V_- , V_+) supported by a fused glass matrix (G). The sensor averages conductivity over a bipolar volume of radial extent ~ 3 mm and has a -3 dB power attenuation near $k \sim 300$ cpm. (Photographs courtesy Mike Head, Precision Measurement Engineering.)

inertial range scaling
IC / VC subranges

viscous-diffusive range scaling

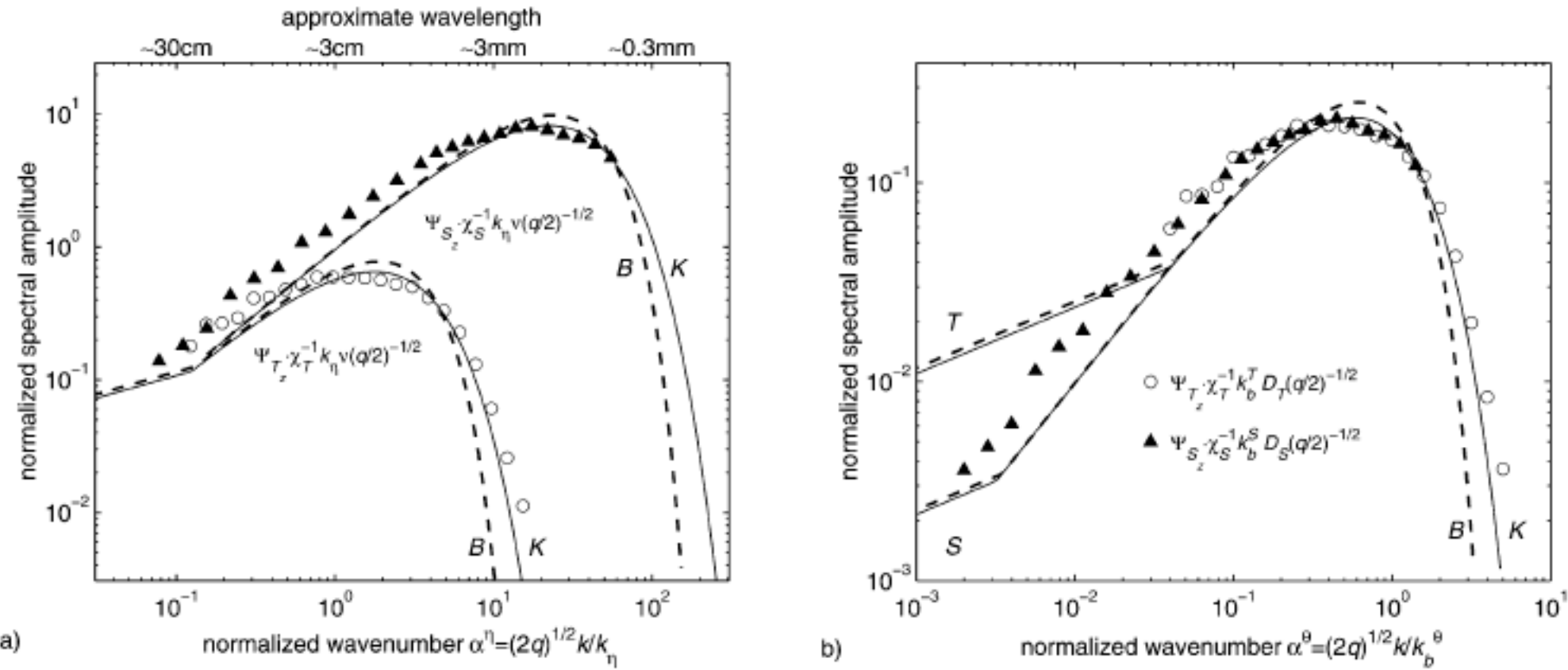


FIG. 11. Collapse of salinity (\blacktriangle) and temperature (\circ) gradient spectra in the viscous-convective (a) and viscous-diffusive (b) subranges is accomplished by appropriate normalization. In (a) both Ψ_{S_z} and Ψ_{T_z} are nondimensionalized with respect to the Kolmogorov wavenumber k_η and molecular viscosity ν , which collapses the low-wavenumber inertial and viscous-convective subranges. In (b) Ψ_{S_z} and Ψ_{T_z} are nondimensionalized by their respective Batchelor wavenumbers (k_b^S or k_b^T) and molecular diffusivities (D_S or D_T), which collapses the spectra in the high-wavenumber viscous-diffusive subrange. The dashed and solid curves represent the universal forms of Batchelor and Kraichnan. Note that the $k^{1/3}$ inertial subrange has a different level and transition wavenumber for each scalar under the latter normalization.